Supplementary Information

Retention and mobility of phosphogypsum constituents in carbonate aquifer rock materials

Nitai Amiel[1], Han Zhang[1], Ishai Dror[1], and Brian Berkowitz[1]

[1]Department of Earth and Planetary Sciences, Weizmann Institute of Science

* Corresponding author: Ishai Dror ishai.dror@weizmann.ac.il

S1. Modified Sequential Extraction Procedure

The sequential extraction procedure was adapted from Scheplitz et al. (2021) to accommodate the high carbonate content of the Zafit aquifer rock. The reagent-to-sample ratios were increased to ensure complete dissolution of the carbonate phase. The extraction was performed on bulk rock samples (before the experiment) and column inlet samples (after the experiment). The five extracted phases are:

1. **Adsorbed/exchangeable:** $MgCl_2$ (1M, pH 7).
2. **Carbonates:** NaOAc (1M) adjusted to pH 5.
3. **Hydrous iron oxides:** $NH_2OH{\cdot}HCl$ (0.04 M) in 25% (v/v) HOAc.
4. **Crystalline iron oxides:** $NH_2OH{\cdot}HCl$ (0.25 M) in HCl (0.25 M).
5. **Sulfides/organic material:** $KClO_3$ and HCl.

S2. Supplementary Tables

Table S1*. The concentration of representative elements in the experimental PGL solution*

Element	**Concentration** mg/L	**Element**	**Concentration** µg/L	**Element**	**Concentration** µg/L
Na	649	Ge	12	La	8.04
K	93	Al	530	Ce	1.10
Mg	163	Rb	140	Pr	4.90
Ca	817	Tl	3.5	Nd	3.52
Cl	629	Cd	300	Sm	2.81
Br	8.7	Cu	130	Gd	1.59
SO_4 (S)	267 (89)	U	210	Tb	2.95
PO_4 (P)	7535 (2405)	Cs	8	Dy	1.78
F	1797	Mo	12	Ho	2.0
Mn	1.2	Cr	72	Er	1.41
Zn	2.6	B	910	Tm	1.19
Ni	1.25	Ba	35	Yb	0.69
---	---	Co	12	Lu	2.44

Table S2. *Bulk composition of the aquifer rock of the Zafit formation (mg element/kg rock)*

Element	Concentration	Element	Concentration	Element	Concentration
Na	1,589±346	Ge	0.184±0.02	La	2.50±0.1
K	760.03±23	Al	1971±83	Ce	5.15±0.3
Mg	553,256±56	Rb	3.84±0.1	Pr	0.62±0.02
Ca	221,777±91	Tl	0.03±0.005	Nd	2.570±0.4
Ti	88±7	Cd	0.99±0.03	Sm	0.75±0.08
V	79±0.2	Cu	14.8±2	Gd	0.48±0.06
Sc	0.38±0.06	U	8.9±2	Tb	0.05±0.01
P	172±8	Cs	0.41±0.05	Dy	0.52±0.05
Sr	668±41	Mo	1.07±0.2	Ho	0.084±0.01
Fe	9,537±327	Cr	9.2±1	Er	0.33±0.06
Mn	1207±32	B	21.5±3	Tm	0.07±0.004
Zn	58.5±3	Ba	140±9	Yb	0.12±0.02
Ni	24.2±1	Co	6.6±1	Lu	0.09±0.005

Table S3. *Detailed experimental conditions of batch and column experiments*

Parameter	Batch Experiments	Column Experiments
Rock material	Zafit dolomite	Zafit dolomite
Grain size	2-5 mm	1-2 mm,2-5 mm,5-10 mm (separate)
Rock mass	10 g	~65-80 g (packed column)
Solution volume	0.5 L (50:1 L:g ratio)	~65-78 mL pore volume
Solution type	3× diluted PGL, pH 3	3× diluted PGL, pH 3
Temperature	Room temperature (~23°C)	Room temperature (~23°C)
Duration	52 days	60 h PGL flow + 12 h DDW rinse
Flow rate	Rotating table mixing	0.60±0.02 mL/min (upward)
Flow geometry	Static batch mixing	Vertical (bottom-up)
Saturation pre-treatment	N/A	24 h DDW, 0.1±0.01 mL/min
Replicates	2	2 per grain size (n=6 total)
Sampling frequency	Hourly → daily	Continuous effluent collection

Table S4. *Saturation indexes of PGL-related elements in pH 3-5 calculated using Visual MINTEQ 3.1*

Mineral	pH 3	pH 4	pH 5
(UO2)3(PO4)2(s)	-15.95	-15.489	-12.547
(VO)3(PO4)2(s)	-28.066	-27.288	-24.292
Ag2MoO4(s)	-14.533	-13.21	-12.932
Ag2O(s)	-25.005	-23.025	-21.033
Ag2Se(s)	8.862	8.87	8.874
Ag2SO4(s)	-16.275	-16.237	-16.222
Ag3AsO3(s)	-25.206	-22.225	-19.233
Ag3PO4(s)	-23.635	-21.623	-19.634
AgF:4H2O(s)	-11.454	-11.131	-11.04
Anglesite	-3.296	-3.467	-3.552
Anhydrite	-1.043	-1.033	-1.041
Arsenolite	-7.425	-7.403	-7.393
Autunite	-11.431	-9.811	-6.546
Avicennite	-17.437	-11.475	-5.499
Ba(OH)2:8H2O(s)	-24.54	-22.566	-20.66
BaF2(s)	-2.499	-1.837	-1.731
BaHPO4(s)	-2.847	-1.82	-0.907
BaMoO4(s)	-6.73	-5.4	-5.203
Barite	1.279	1.323	1.257
Be(OH)2 (alpha)	-15.951	-15.261	-13.635
Be(OH)2 (am)	-16.251	-15.561	-13.935
Be(OH)2 (beta)	-15.551	-14.861	-13.235
BeMoO4(s)	-20.915	-20.881	-20.968
Bianchite	-5.216	-5.356	-5.693
BiOBr(s)	1.941	2.738	2.72
BiOCl(s)	4.494	5.293	5.276
Bromyrite	-0.516	-0.518	-0.518
Brucite	-13.861	-12.116	-10.246

Mineral	pH 3	pH 4	pH 5
Ca3(PO4)2 (am1)	-9.875	-5.937	-2.025
Ca3(PO4)2 (am2)	-7.125	-3.187	0.725
Ca3(PO4)2 (beta)	-6.455	-2.517	1.395
Ca4H(PO4)3:3H2O(s)	-6.785	-1.858	3.022
CaHPO4(s)	-0.049	0.944	1.914
CaHPO4:2H2O(s)	-0.353	0.637	1.606
CaMoO4(s)	-2.442	-1.147	-0.892
Cd(BO2)2(s)	-30.107	-24.939	-18.309
Cd(OH)2(s)	-13.787	-11.93	-10.361
Cd3(OH)4SO4(s)	-31.642	-28.011	-25.281
Cd3(PO4)2(s)	-12.951	-9.292	-6.58
Cd3OH2(SO4)2(s)	-24.443	-22.753	-22
Cd4(OH)6SO4(s)	-37.625	-32.137	-27.839
CdBr2:4H2O(s)	-10.955	-11.086	-11.512
CdCl2(s)	-8.266	-8.388	-8.809
CdCl2:1H2O(s)	-7.244	-7.367	-7.789
CdCl2:2.5H2O(s)	-7.042	-7.167	-7.59
CdF2(s)	-7.201	-6.667	-6.902
CdMoO4(s)	0.366	1.568	1.423
CdOHCl(s)	-8.071	-7.204	-6.63
CdSe(s)	-7.339	-7.452	-7.87
CdSO4(s)	-8.623	-8.706	-9.114
CdSO4:1H2O(s)	-7.081	-7.166	-7.574
CdSO4:2.67H2O(s)	-6.954	-7.041	-7.451
Ce(OH)3(s)	-21.987	-19.243	-16.326
CeF3(s)	4.598	5.358	5.568
Celestite	-1.083	-1.061	-1.076
CePO4(s)	1.642	3.43	5.35

Mineral	pH 3	pH 4	pH 5
Cerargyrite	-0.862	-0.862	-0.862
Chloropyromorphite(c)	0.186	5.176	10.645
Chloropyromorphite(soil)	-3.844	1.146	6.615
Claudetite	-7.465	-7.443	-7.433
Clausthalite	-2.73	-2.93	-3.026
Co(BO2)2(s)	-47.493	-42.371	-35.553
Co(OH)2 (am)	-13.393	-11.582	-9.825
Co(OH)2 (c)	-12.589	-10.778	-9.021
Co3(PO4)2(s)	-11.329	-7.81	-4.533
CoCl2(s)	-17.347	-17.516	-17.749
CoCl2:6H2O(s)	-11.689	-11.865	-12.102
CoF2(s)	-6.972	-6.484	-6.531
CoHPO4(s)	-3.81	-2.958	-2.198
CoMoO4(s)	-6.178	-5.023	-4.979
CoO(s)	-13.873	-12.061	-10.303
CoSe(s)	-11.494	-11.654	-11.883
CoSO4(s)	-11.753	-11.883	-12.102
CoSO4:6H2O(s)	-6.55	-6.688	-6.911
Cotunnite	-6.436	-6.645	-6.744
Cr(OH)3 (am)	-12.456	-10.449	-7.735
Cr2O3 (c)	-24.535	-20.518	-15.088
CrBr3(s)	-52.636	-53.605	-53.879
CrCl3(s)	-41.233	-42.194	-42.466
CrF3(s)	-14.014	-13.991	-13.984
Cu2Se (alpha)	9.926	9.932	9.935
Cu2SO4(s)	-15.18	-15.145	-15.132
CuBr(s)	-2.533	-2.537	-2.538
CuF(s)	-3.469	-3.142	-3.049

Mineral	pH 3	pH 4	pH 5
Cuprite	-7.061	-5.083	-3.093
Dy(OH)3(s)	-18.445	-15.758	-12.843
DyF3(s)	2.83	3.533	3.74
DyPO4(s)	0.285	2.015	3.932
Epsomite	-3.371	-3.576	-3.687
Er(OH)3(s)	-17.924	-15.237	-12.323
ErF3(s)	3.061	3.763	3.971
ErPO4(s)	0.005	1.736	3.653
Fluorite	5.479	6.106	6.27
Ga(OH)3 (am)	-10.21	-8.207	-5.495
GaOOH(s)	-8.098	-6.094	-3.381
GaPO4(s)	-4.94	-3.894	-2.179
Gd(OH)3(s)	-18.672	-16.334	-13.744
GdF3 x H2O (s)	0.907	1.26	1.143
GdF3(s)	2.103	2.457	2.34
GdPO4 x H2O(s)	-1.854	-0.474	1.118
GdPO4(s)	-0.542	0.84	2.432
Goslarite	-4.982	-5.124	-5.461
Gypsum	-0.817	-0.81	-0.82
H2MoO4(s)	-0.788	-1.446	-3.161
H2WO4(s)	-1.495	-1.809	-3.458
Halite	-4.499	-4.514	-4.524
H-Autunite	-10.7	-11.033	-9.738
HfO2(s)	-0.623	2.436	3.377
Ho(OH)3(s)	-18.022	-15.335	-12.421
HoF3(s)	2.353	3.056	3.263
HoPO4(s)	0.208	1.938	3.855
Hydroxyapatite	-7.105	-0.223	6.629

Mineral	pH 3	pH 4	pH 5
Hydroxylpyromorphite	-17.063	-11.084	-4.619
K2MoO4(s)	-16.155	-14.852	-14.58
K-Autunite	-9.615	-7.987	-4.706
KCl(s)	-4.917	-4.927	-4.93
La(OH)3(s)	-21.294	-18.491	-15.549
LaF3(s)	5.292	6.11	6.346
LaPO4(s)	2.186	4.033	5.978
Larnakite	-13.074	-11.474	-9.667
Laurionite	-7.448	-6.668	-5.772
Li2MoO4(s)	-18.751	-17.483	-17.28
LiF(s)	-2.7	-2.399	-2.343
Lime	-29.439	-27.487	-25.518
Litharge	-15.112	-13.341	-11.449
Lu(OH)3(s)	-17.352	-14.665	-11.751
LuF3(s)	1.523	2.225	2.433
LuPO4(s)	-0.123	1.608	3.525
Massicot	-15.312	-13.541	-11.649
Matlockite	-1.987	-1.868	-1.874
Mg(OH)2 (active)	-15.555	-13.81	-11.94
Mg2(OH)3Cl:4H2O(s)	-23.962	-21.466	-18.724
Mg3(PO4)2(s)	-12.124	-8.802	-5.188
MgCr2O4(s)	-38.805	-33.041	-25.741
MgF2(s)	3.079	3.501	3.566
MgHPO4:3H2O(s)	-1.195	-0.412	0.458
MgMoO4(s)	-8.552	-7.462	-7.306
Mirabilite	-4.774	-4.781	-4.792
MoO3(s)	-5.652	-6.309	-8.023
Na2Mo2O7(s)	-7.812	-7.177	-8.633
Na2MoO4(s)	-12.246	-10.954	-10.696
Na2MoO4:2H2O(s)	-12.004	-10.715	-10.458
Na-Autunite	-8.313	-6.696	-3.428
NaF(s)	-2.203	-1.89	-1.807

Mineral	pH 3	pH 4	pH 5
Nantokite	-1.9	-1.901	-1.902
Nd(OH)3(s)	-19.703	-17.015	-14.1
NdF3(s)	6.282	6.986	7.194
NdPO4(s)	2.027	3.758	5.676
Pb(BO2)2(s)	-29.078	-23.996	-17.045
Pb(OH)2(s)	-10.585	-8.815	-6.923
Pb2(OH)3Cl(s)	-18.053	-15.503	-12.715
Pb2O(OH)2(s)	-31.047	-27.506	-23.723
Pb3(PO4)2(s)	-8.894	-5.497	-1.818
Pb3O2SO4(s)	-26.617	-23.246	-19.548
Pb4(OH)6SO4(s)	-39.49	-34.351	-28.763
Pb4O3SO4(s)	-40.231	-35.088	-29.498
PbBr2(s)	-10.323	-10.536	-10.637
PbBrF(s)	-4.674	-4.557	-4.564
PbF2(s)	-3.264	-2.817	-2.731
PbHPO4(s)	-1.202	-0.39	0.503
PbMoO4(s)	-0.455	0.659	0.837
PbO:0.3H2O(s)	-15.406	-13.636	-11.744
Periclase	-18.333	-16.587	-14.717
Portlandite	-19.455	-17.505	-15.536
Powellite	-2.472	-1.177	-0.922
Pr(OH)3(s)	-20.88	-18.191	-15.277
PrF3(s)	6.396	7.1	7.308
PrPO4(s)	2.451	4.183	6.1
Przhevalskite	-16.676	-15.237	-12.049
Rutile	4.39	4.442	4.451
Saleeite	-11.722	-10.307	-7.141
Sb2O3 (s)	-8.631	-7.297	-5.592
Sb2Se3(s)	-31.576	-36.157	-40.415
Sb4O6 (cubic)	-15.663	-12.995	-9.584
Sb4O6 (rhombic)	-16.513	-13.845	-10.434
SbBr3(s)	-29.325	-31.635	-33.771

Mineral	pH 3	pH 4	pH 5
SbCl3(s)	-22.318	-24.621	-26.755
SbF3(s)	-10.753	-12.073	-13.928
Scheelite	-4.902	-3.264	-2.942
Schoepite	-12.145	-11.355	-9.71
ScOOH(s)	-24.639	-22.98	-20.366
Senarmontite	-5.671	-4.337	-2.632
Sm(OH)3(s)	-18.183	-15.495	-12.58
SmF3(s)	4.992	5.696	5.904
SmPO4(s)	1.837	3.569	5.486
Sn(OH)2(s)	-9.225	-8.226	-6.513
SnBr2(s)	-17.769	-18.753	-19.033
SnCl2(s)	-13.632	-14.611	-14.889
SnO(s)	-8.813	-7.813	-6.099
SnSe(s)	-11.027	-11.997	-12.272
SnSO4(s)	34.198	33.256	32.992
Sr-Autunite	-13.201	-11.569	-8.311
SrF2(s)	1.259	1.898	2.056
SrHPO4(s)	-2.329	-1.324	-0.36
Tb(OH)3(s)	-17.75	-15.063	-12.149
TbF3(s)	3.525	4.228	4.435
TbPO4(s)	0.769	2.5	4.417
Thenardite	-6.089	-6.082	-6.088
Tl(OH)3(s)	-9.796	-6.816	-3.829
TmF3(s)	2.069	2.771	2.979
TmPO4(s)	-0.177	1.554	3.471
UO2(OH)2 (beta)	-12.355	-11.564	-9.918
UO2HPO4(s)	-5.09	-5.257	-4.609
UO3(s)	-14.431	-13.639	-11.992
Uranocircite	-14.025	-12.371	-9.164
V2O4(s)	-6.94	-6.041	-4.377
Valentinite	-7.111	-5.777	-4.072
VF4(s)	-34.164	-35.914	-37.86

Mineral	pH 3	pH 4	pH 5
VO(OH)2(s)	-8.572	-7.675	-6.011
VOCl2(s)	-24.224	-25.305	-25.632
VOSO4(s)	-14.943	-15.987	-16.3
Y(OH)3(s)	-23.801	-21.806	-19.095
Yb(OH)3(s)	-18.284	-15.615	-12.856
YbF3 x H2O (s)	0.695	1.379	1.43
YbF3(s)	0.991	1.676	1.727
YbPO4 x H2O(s)	-1.367	0.345	2.105
YbPO4(s)	-0.554	1.158	2.919
YF3 x H2O (s)	-1.822	-1.812	-1.808
YF3(s)	-0.416	-0.405	-0.401
YPO4 x H2O(s)	-4.683	-3.646	-1.933
YPO4(s)	-3.851	-2.813	-1.099
Zincite	-9.475	-7.665	-6.021
Zincosite	-10.838	-10.971	-11.304
Zn(BO2)2(s)	-26.671	-21.551	-14.847
Zn(OH)2 (am)	-10.731	-8.923	-7.279
Zn(OH)2 (beta)	-10.011	-8.203	-6.559
Zn(OH)2 (delta)	-10.101	-8.293	-6.649
Zn(OH)2 (epsilon)	-9.791	-7.983	-6.339
Zn(OH)2 (gamma)	-9.991	-8.183	-6.539
Zn2(OH)2SO4(s)	-12.666	-10.989	-9.679
Zn2(OH)3Cl(s)	-16.096	-13.468	-11.177
Zn3(PO4)2:4H2O(s)	-4.52	-1.013	1.92
Zn3O(SO4)2(s)	-30.976	-29.43	-28.453
Zn4(OH)6SO4(s)	-30.079	-24.787	-20.19
Zn5(OH)8Cl2(s)	-38.566	-31.503	-25.277
ZnCl2(s)	-14.088	-14.259	-14.606
ZnF2(s)	-5.992	-5.507	-5.668
ZnMoO4(s)	-1.772	-0.619	-0.689
ZnSe(s)	-11.252	-11.414	-11.758
ZnSO4:1H2O(s)	-6.283	-6.416	-6.75

Table S5. *Saturation indexes of PGL-related elements in pH 3-5 calculated using Visual MINTEQ 3.1*

pH	Mo Total Aqueous (%)	Mo as MoO_4^{2-} (%)	Ge Total Aqueous (%)	Ge as $H_3GeO_3^0$ (%)	Ge as $H_2GeO_3^-$ (%)	SI Mo Precipitation	SI Ge Precipitation
3.0	98.5	97.2	98.8	85.2	12.1	-2.1	-3.2
4.0	99.2	98.8	99.1	78.4	18.9	-1.8	-3.0
5.0	99.5	99.3	98.9	65.3	31.2	-1.6	-2.8
5.7	99.7	99.6	98.5	58.1	38.4	-1.4	-2.6

Table S6. *Visual MINTEQ Model Inputs and Parameters*

Parameter Category	Input Value/Setting	Experimental Match
Software Version	Visual MINTEQ 3.1	-
Temperature	25°C	Matches room temperature experiments (~23°C)
Solution Composition	Measured PGL (3× diluted): Na^+: 649 mg/L Ca^{2+}: 817 mg/L Cl^-: 629 mg/L P: 2405 mg/L F^-: 1797 mg/L 39 trace elements	Direct from ICP-MS analysis (Table S1)
Ionic Strength	0.08–0.15 M (Davies equation)	Calculated from measured ion concentrations during batch/column experiments
pH Range	3.0–5.7	Initial pH 3.0 → final batch pH 5.7 (Fig. 1P); column pH 3.0→4.5
Thermodynamic Database	MINTEQ3.1 (default)	Default complexation constants for all aqueous species
Allowed Solid Phases	- Carbonates: dolomite ($CaMg(CO_3)_2$), calcite ($CaCO_3$) - Phosphates: hydroxyapatite ($Ca_{10}(PO_4)_6(OH)_2$), $CaHPO_4$ - Fluorides: CaF_2 (fluorite), MgF_2 - REE minerals: $REPO_4$, REF_3 - Hydroxides: $Al(OH)_3$, $Cr(OH)_3$, $Cu(OH)_2$, $Zn(OH)_2$, $Cd(OH)_2$, $Ni(OH)_2$	Matches Zafit rock minerals (Fig. S1), secondary precipitates (Figs. S3,S6), post-column rock (Fig. S8)
Major Ligands	$PO_4^{3-}/HPO_4^{2-}/H_2PO_4^-$, F^-/HF, SO_4^{2-}/HSO_4^-, Cl^-, CO_3^{2-}/HCO_3^-	Dominant anions in measured PGL (Table S1)
Organic Matter	Excluded	PGL is mineral leachate (no NOM detected)
Model Assumptions	Thermodynamic equilibrium (no kinetics)	Validated for 52-day batch timescale; SI > 0 predicts observed precipitation

S3. Supplementary Figures

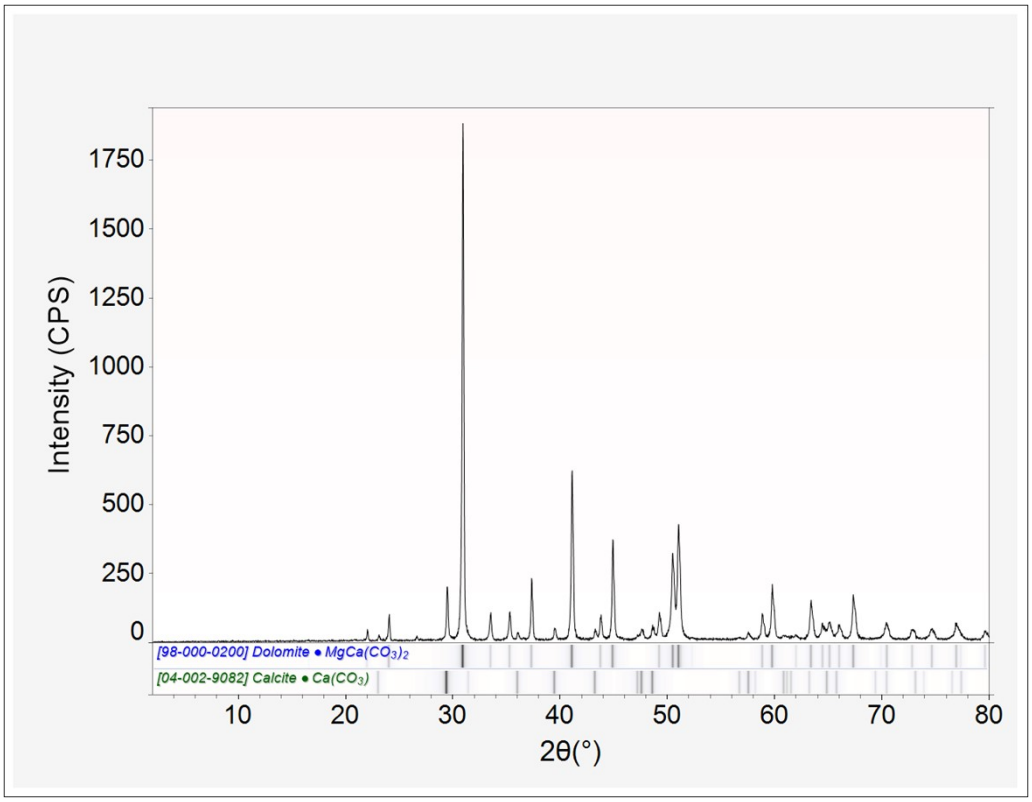

Figure S1. *XRD of the Zafit rock sample and its fit to dolomite and calcite standards.*

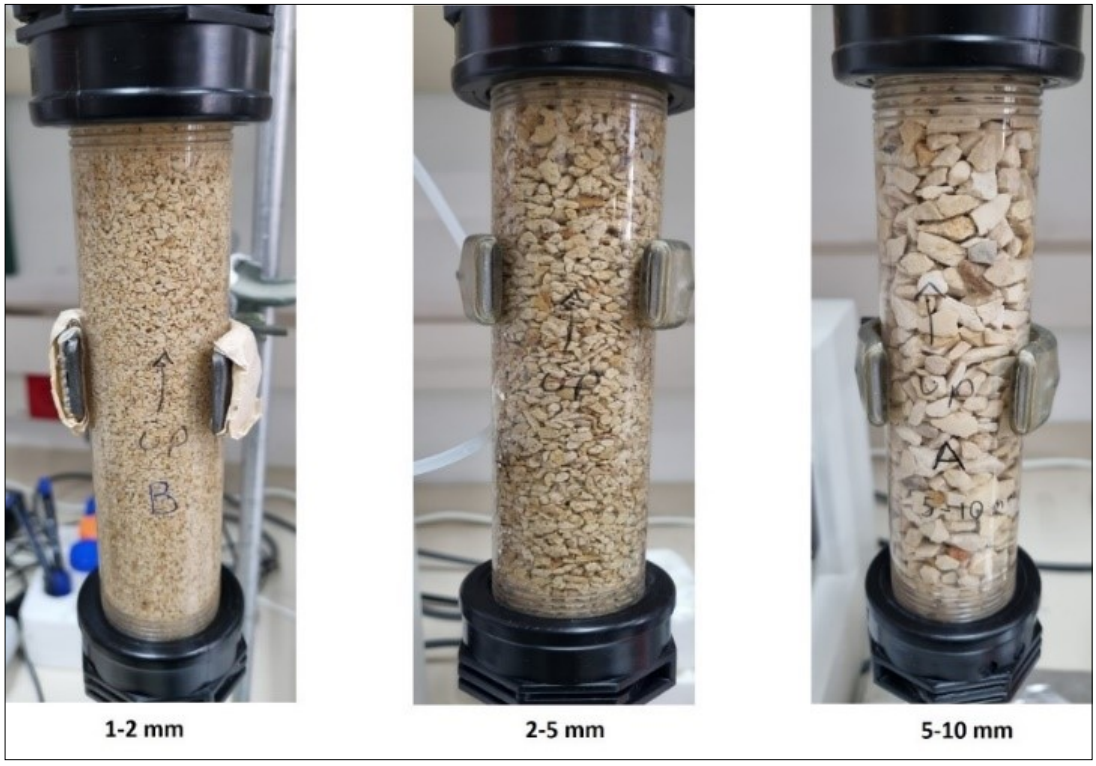

Figure S2. *Columns packed with dolomite aquifer rock in three different grain sizes.*

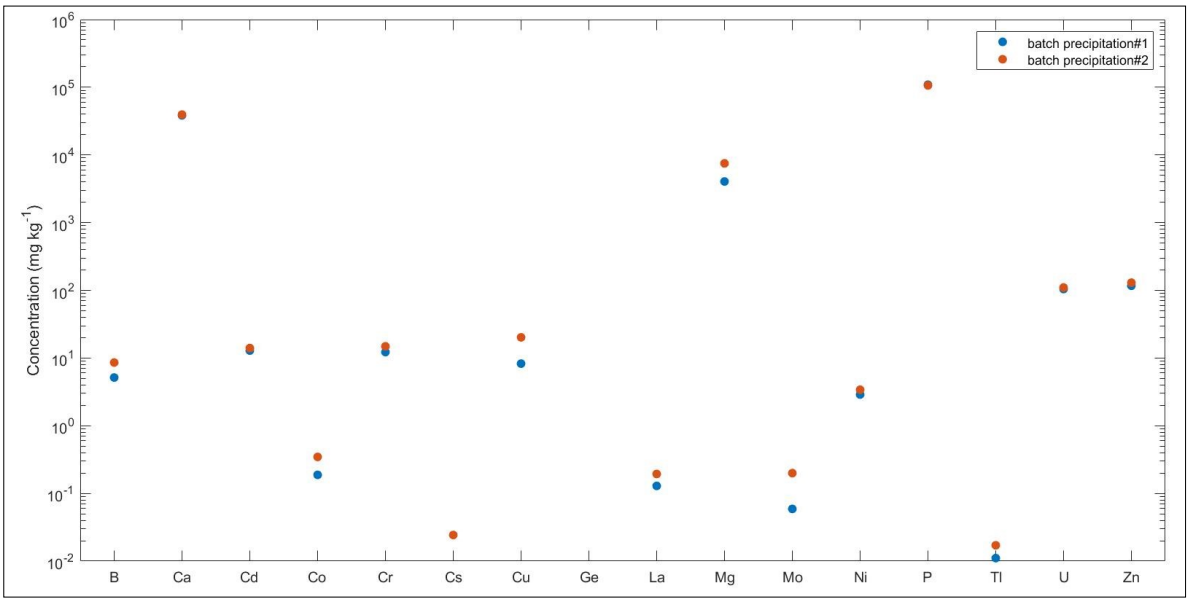

Figure S3. *Concentrations of elements in the dissolved fraction of the newly precipitated minerals in the batch experiment. Colors represent replicates extracted from the batch experiment solution.*

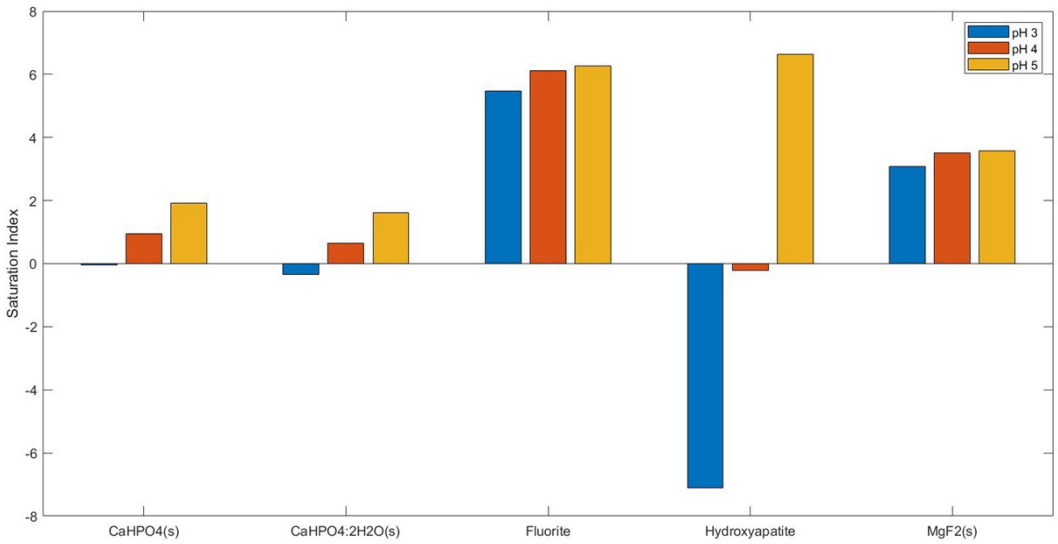

Figure S4. *Saturation indexes of Ca and Mg minerals in solution in pH 3-5. Calculated using Visual MINTEQ 3.1.*

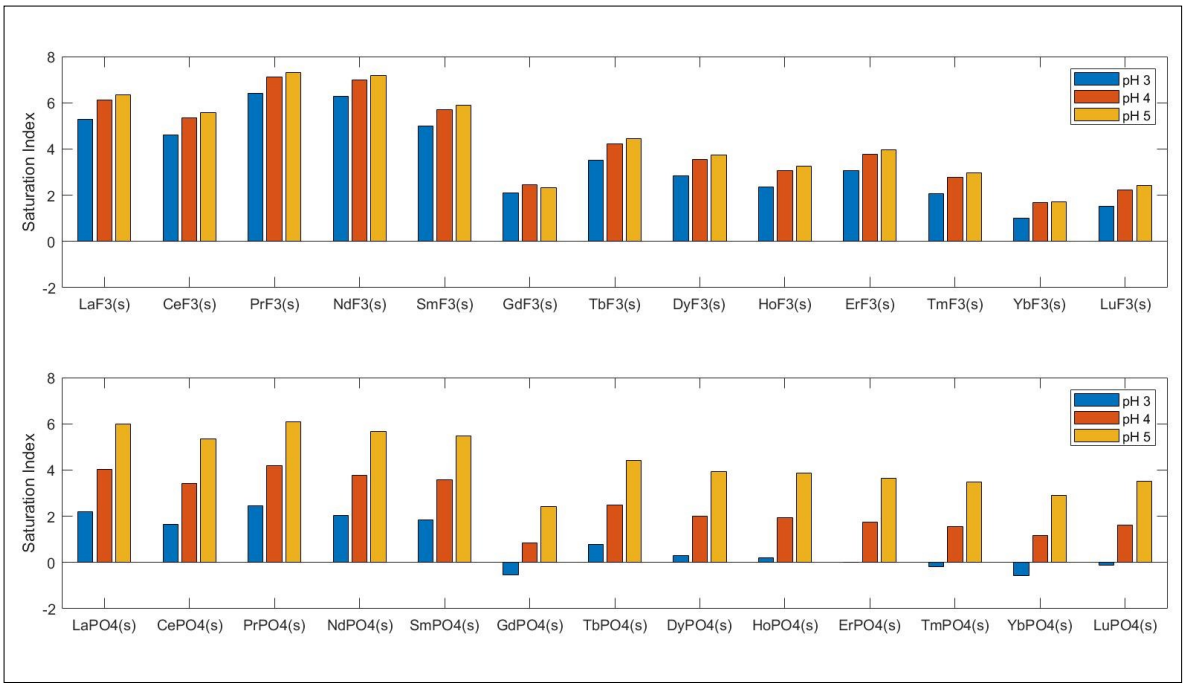

Figure S5. *Saturation indexes of REE-F3 minerals (upper panel) and REE-PO4 (lower panel), calculated using Visual MINTEQ 3.1.*

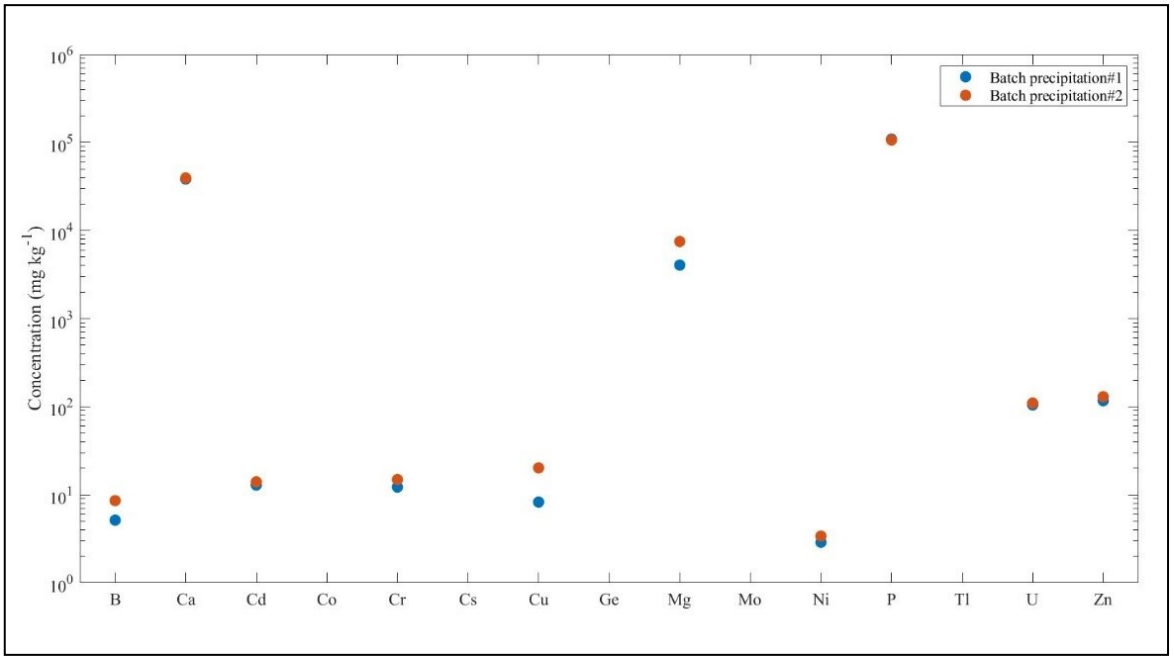

Figure S6. *Concentrations of elements in the dissolved fraction of the newly precipitated minerals in the batch experiment. The different colors represent the two replicates extracted from the batch experiment solution.*

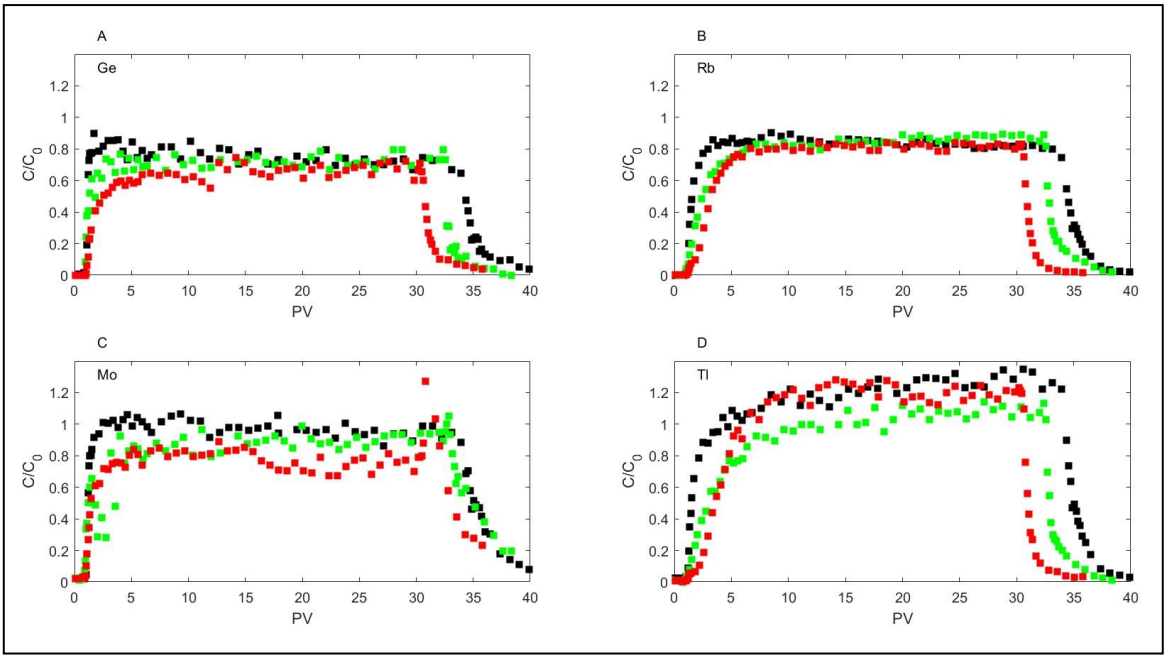

Figure S7. *BTC of elements with little interaction with the rock. Black symbols: 5-10 mm grain. Green symbols: 2-5 mm grains. Red symbols: 1-2 mm grain. These elements of BTCs and recoveries were similar through the different grain-size column experiments.*

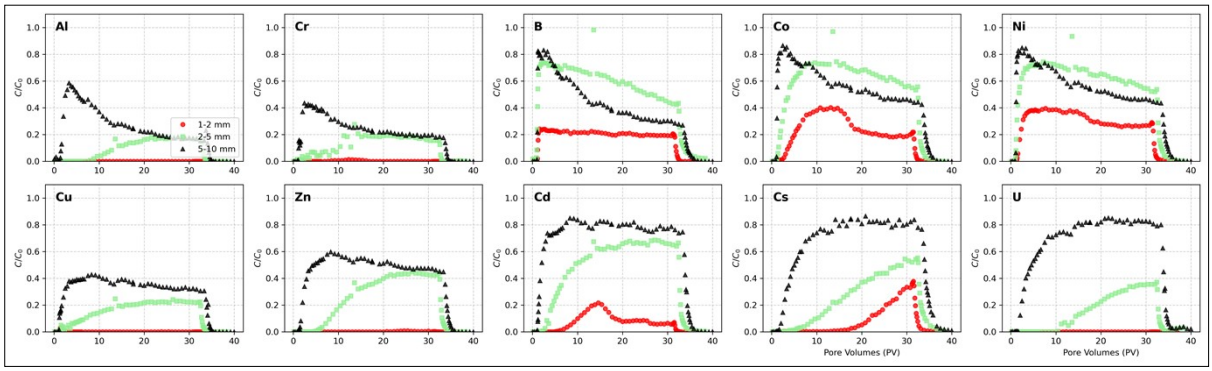

Figure S8. *Replicate of Panels in Figure 3 F-O*

S4. Calculation of Solid Retention Efficiency

Retention efficiency (η) was calculated directly from aqua regia digestions of inlet rock slices (0–2 cm, ~13 g dry mass) versus initial bulk rock, extrapolated to total column dry rock mass (188 g):

$$\eta(\%) = 100 \times \frac{(C_{initial} - C_{post}) \times m_{total}}{C_{inlet} \times V_{inlet}}$$

where:

- $(C_{initial} - C_{post})$: post-experiment/initial rock concentration (µg/g).
- m_{total}= 188 g (full column).
- C_{inlet} : PGL input concentration (µg/L, Table S1).
- V_{inlet}=2160 mL (60 h × 0.6 mL/min PGL phase).

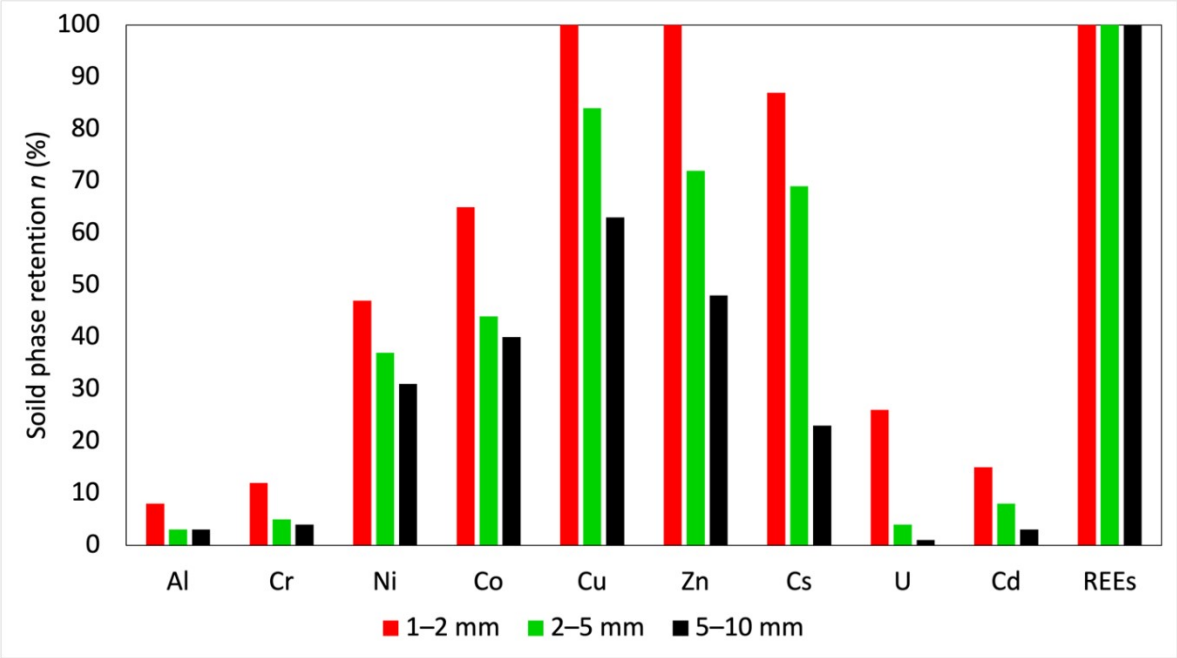

Figure S9*. Solid phase retention of representative elements. Retention increases with decreased grain size.*

S5. Elemental Concentration prior to and after the PPG column experiment

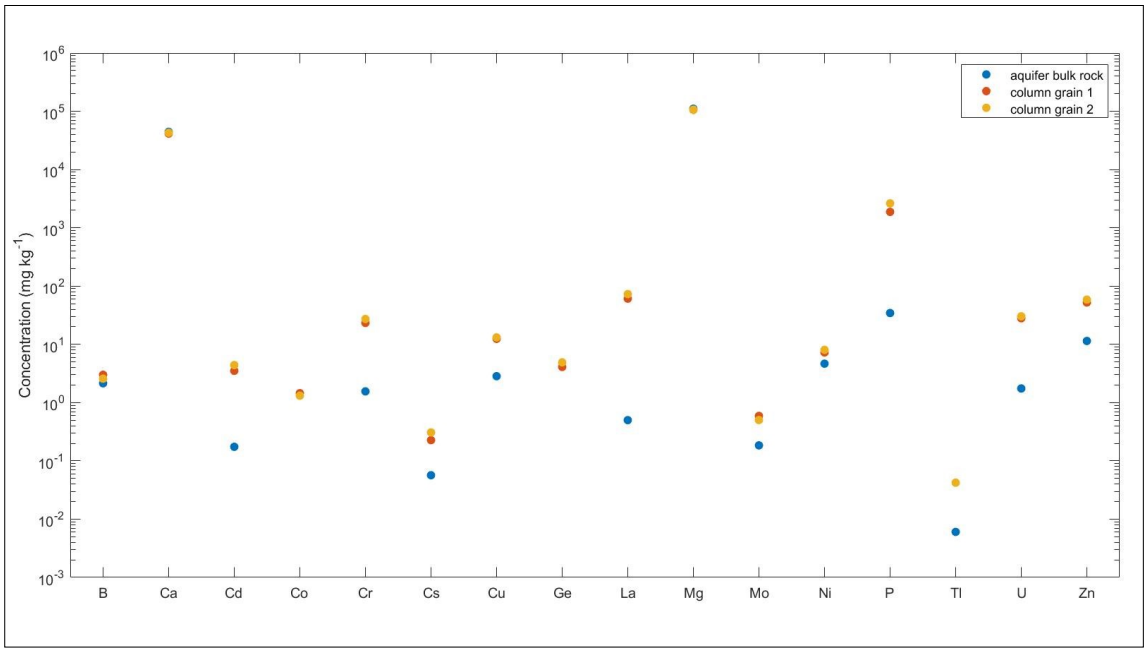

Figure S10. *The concentration of different elements on the aquifer rock grain was obtained from the column inlet prior to (blue dots) and after (red and yellow dots) the PPG column experiment.*

Figure S10 indicates that the initial carbonate aquifer rock (blue) contains lower solid-phase concentrations than the post-PPG reacted material for all reported elements, including Cd, Cr, Cs, Cu, La, Mo, Ni, P, U, Zn, and Tl. No element shows an opposite trend. While the *y*-axis is logarithmic, the key observation remains robust: reaction with the experimental solution yields a reacted solid systematically enriched relative to the starting rock. Tl displays the smallest enrichment on an absolute scale (mg kg^{-1}), implying that Tl is least effectively transferred from solution back to the solid during reaction.

A coherent mechanistic explanation involves two coupled processes: selective dissolution of carbonate minerals and element-specific repartitioning during fluid–rock interaction. Acidic influent promotes carbonate dissolution through proton consumption, buffering the fluid and increasing alkalinity. This buffering changes metal speciation and shifts the balance between dissolved and solid-associated forms. Many metals partition strongly to carbonate-bearing media as pH rises, via surface complexation on carbonate and accessory phases, adsorption onto newly generated surfaces, and coprecipitation with secondary carbonates or Fe/Mn oxyhydroxides if such phases are present or form during reaction. These pathways enrich the residual solid in trace elements, even as dissolution removes a fraction of the carbonate matrix.

Tl often behaves differently because it can remain relatively soluble across a broad pH range and may exhibit weaker affinity for carbonate surfaces compared with transition metals and some oxyanion-forming elements. Under these conditions, Tl uptake into the solid is limited, producing only modest solid-phase enrichment relative to the pronounced enrichments observed for the other elements.

The implication for Tl sourcing is straightforward. Because the influent solution was Tl-free, the Tl observed in the breakthrough curve must originate from the solid. The low Tl enrichment of the reacted solid further suggests limited recapture during buffering, consistent with Tl being released during carbonate dissolution and transported predominantly in the dissolved phase. Taken together, these observations support carbonate rock dissolution as the dominant Tl source responsible for the observed BTC.

S6. Sequential Extraction Results

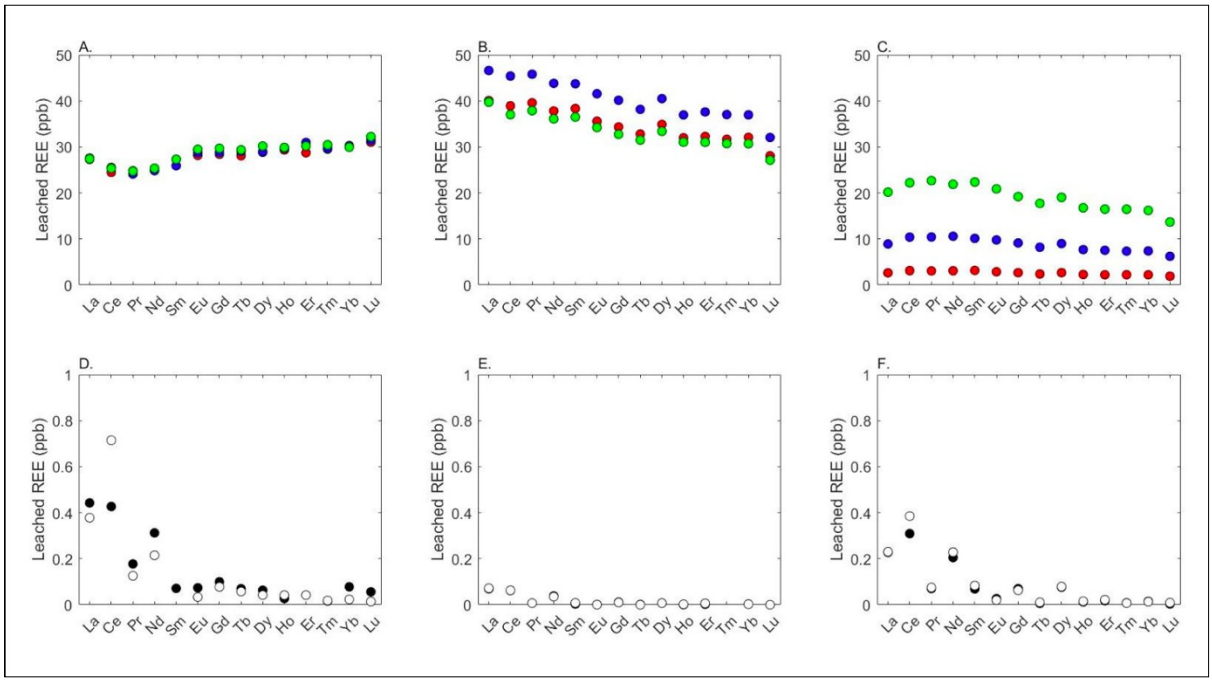

Figure S11. *Sequential extraction results comparing REE fractionation in the pristine Zafit aquifer rock (Before Experiment) versus rock grains obtained from the column inlet (After Experiment). (A-C) Concentration of REEs in the post-experiment rock grains. (D-F) Background concentration of REEs in the pristine bulk rock. The comparison highlights a significant net accumulation of REEs in Step 2 (Carbonates), Step 3 (Hydrous iron oxides), and Step 4 (Crystalline iron oxides) following exposure to PGL. Note: Concentrations in Step 1 (Adsorbed/exchangeable) were negligible (<1 μg* L^{-1}*) in both cases.*